A precision capacitance cell for measurement of thin film out-of-plane expansion. I. Thermal expansion

Chad R. Snyder and Frederick I. Mopsik[a)]
NIST, Polymers Division, Gaithersburg, Maryland 20899

(Received 9 June 1998; accepted for publication 17 August 1998)

A high sensitivity technique based on a three-terminal parallel plate capacitor for the measurement of the out-of-plane expansion of thin films is presented. The necessary assembly protocols and data reduction techniques for the proper use of this capacitance cell are presented. To demonstrate the ability of the technique to produce correct results for the thermal expansion of materials, the results on $\langle 0001 \rangle$ single crystal Al_2O_3 are shown and compared to the literature. Also, results for a thin polymeric film designed for use as an interlayer dielectric are shown to display the utility of the technique to resolve the measurement of displacement in thin films. [S0034-6748(98)03011-1]

I. INTRODUCTION

One of the key design parameters in the microelectronics industry is the coefficient of thermal expansion (CTE). CTE mismatch between different materials is a prime concern due to the fact that thermal stresses can build up as a result and lead to device failure. It is therefore vitally important that reliable values for the CTE of the materials be known so that modeling can be performed to assist design of the structure to minimize the chances of such failures. The materials used in these structures are often in the form of thin films. The CTE value for these materials is often obtained from measurements performed on large (thick) samples. However, many of these materials can be formed only as thin layers and there is some question in the literature regarding the thickness dependence of the CTE.[1–3] The measurement of the thermal expansion of those thin materials in the thickness direction presents a special challenge since the displacements are so small. For a 25 μm thick film with a coefficient of thermal expansion (α):

$$\alpha = \frac{1}{l}\frac{dl}{dT} \tag{1}$$

of $10^{-4}\,\mathrm{K}^{-1}$, a change of 10 °C produces a displacement of 25 nm. In the above equation, l is the sample length/thickness and T is the temperature. Since the coefficient of thermal expansion is expected to be temperature dependent, a relative expanded uncertainty in the change in thickness of $\pm 1\%$ over the 10 °C interval requires resolution beyond the capability of most displacement gauges.

Thermomechanical analysis (TMA), a displacement gauge based technique, is the current technique that is widely utilized by industry for determination of the CTE of solid materials. The limitation of TMA is readily seen by reviewing the American Society for Testing and Materials (ASTM) technique E831-93 which calls for sample dimensions between 2 and 10 mm.[4]

One method that, in principle, offers the necessary resolution is the measurement of the capacitance between a pair of plane-parallel plates. The capacitance of an ideal 5 cm diam pair of electrodes with a spacing of 25 μm in vacuum is 700 pF, a magnitude that can be measured to a relative standard uncertainty of better than 10^{-6} pF/pF with commercial instrumentation. If the sample can be used to determine the spacing between the plates (d), such that the sample is not in the measuring circuit, for a constant effective area of the plates A, the capacitance in a vacuum C_{vac} is given by:

$$C_{\mathrm{vac}} = \frac{\epsilon_0 A}{d}, \tag{2}$$

where ϵ_0 is the permittivity of free space ($\epsilon_0 = 8.854\,\mathrm{pF/m}$). The resolution in thickness d then becomes the resolution in capacitance directly and the required precision in length can be achieved. Since capacitance can be measured over a very wide range of values to high precision with modern three-terminal bridges, the relative expanded uncertainty of the measurement is independent of the sample thickness for a wide range of separations.

II. EARLY ATTEMPTS AND CLAIMS

Capacitance cell methods come in two general types: two-terminal and three-terminal methods. Of the two, the three-terminal method has the least uncertainties. The capacitance cell of Sao and Tiwary[5] was a two-terminal method that suffered from the problem of alignment of the electrodes plus expansion of the electrodes. The three-terminal method of Subrahmanyam and Subramanyam[6] suffers from several problems: electrode alignment, expansion, and contraction of the entire apparatus, and the thermal spring constant which determines the loading conditions. The design of Tong and co-workers[7] required careful alignment as it was a two-terminal design and did not use a guard ring to help define the area. This also made it susceptible to stray capacitances and other fluctuations. Ho and co-workers present results obtained through the use of their capacitance cell and state a resolution of 2 Å.[3] However, no design information or error

a)Electronic mail: fim@nist.gov

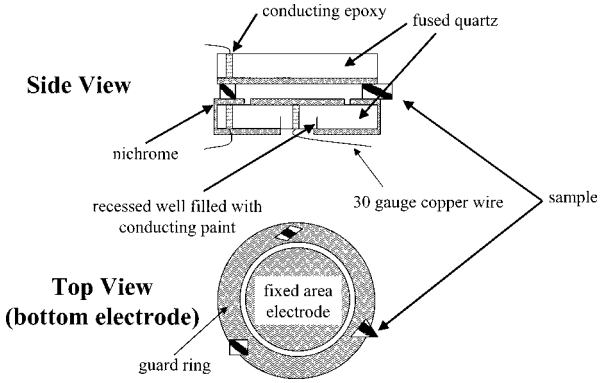

FIG. 1. Schematic of capacitance cell.

analysis is included in their article, and the article which is referenced in their work for such information (a Semiconductor Research Corporation conference proceeding) is unavailable to the general public.

If a three-terminal guarded electrode is properly constructed, the electrode area to be used in Eq. (2) is independent of position of the opposite electrode since the area is defined solely by the inner, guarded electrode, as long as the opposing electrode is much larger than the diameter defined by the guard gap.[8] Furthermore, for any easily realized guard gap, the effective area of the electrode varies only very gradually with a change in plate separation. For the changes in length observed in the measurement of thermal expansion, using realizable gaps, the area is nearly an ideal constant to within the limits set by the thermal expansion of the guarded electrode.

Our technique eliminates the problem of electrode alignment and uses the sensitivity of the three-terminal measurement. Previous measurements were reported on an earlier design[9] of our cell made from gold-coated Zerodur.[10,11] The current design addresses the weaknesses discovered in the use of the previous cell and eliminates all systematic errors resulting from the use of the electrodes.

III. EXPERIMENT

A. Electrode design

The electrodes, fabricated from 10 cm blanks of fused quartz, were ground and polished to optical flatness. The top electrode was 1 cm thick and had a small hole drilled in it near the edge so that a 16 gauge wire could be inserted in it and held in place by a conductive epoxy resin that was rated for use up to 350 °C. This hole was positioned so that it was well outside a 6 cm diameter on the blank. The entire flat surface was then coated with a nichrome conductive layer. Since the area of the capacitance is completely determined by the region enclosed by the guard gap on the bottom electrode, the top has no positioning requirements other than it completely overlap the guard gap. Also, while fused quartz was used, any material that can maintain flatness over the temperature range can be used for the top electrode since its area does not affect the measurement.

The bottom electrode was made from a 2 cm thick blank. It is shown in cross section in Fig. 1. It also was polished flat and had two holes drilled: one in the center and the other near the edge, as on the top electrode. Wires were inserted in both holes in the same manner as the top electrode. A nichrome coating was applied such that it covered all surfaces except for a small area around the central wire on the back side. The coating was then removed on a 3 cm radius on the top surface to form a guard gap of minimal cross-sectional area. This created a monolithic guarded electrode assembly whose effective area was defined by the gap so that the capacitance for a 1 mm separation between the top and bottom electrodes was 25 pF.

The main precautions in the electrode fabrication were the maintenance of flatness and the minimization of the guard gap. The leads were recessed slightly so that the epoxy did not interfere with the polishing operation and minimized any effects from thermal expansion in the holes. The gap was scribed in such a way as to minimize any raising of material in its fabrication. This was to allow thinner films to be measured, since any contact between the electrodes will prevent a measurement from being carried out. The limit as to how thin a sample can be used is set mainly by any asperities in the electrode as a nichrome film has almost no contact resistance and any interelectrode contact will act as a direct short circuit.

In the original publication describing the results of the cell, the electrodes were made from Zerodur due to its low coefficient of thermal expansion.[10,11] In that design, any capacitive coupling through the Zerodur was minimized not only by the narrow guard gap but also a continuation of the guard electrode around the back so that it was close to the center contact.

Despite these precautions, there was still a small residual coupling from the central contact through the guard gap to the high electrode that appeared as a temperature dependent thickness error. This can be understood by noting that this coupling is in parallel with the direct high-to-low capacitance and depends directly on variations in the dielectric constant of the blank. Also, careful attempts to model the introduced error showed that it was too complex to be compensated. This problem is made more difficult in Zerodur since the material displayed an apparent ferroelectric behavior as shown in Fig. 2, where the measured dielectric constant (ϵ) using a spare blank was fitted to a Curie–Weiss law with T_C equal to 206 °C. This rapid variation with temperature, if included in the measurement, would create an apparent negative thermal expansion as was revealed in the earlier design. For the samples of interest, it was determined that fused quartz would function as well as the Zerodur, as long as the expansion of the fused quartz electrode was determined. Therefore, it was chosen over the Zerodur to minimize any temperature dependent coupling term.

In addition, this source of error was minimized by improved shielding in the guarded electrode assembly. A thin circular groove about 1 cm in diameter was cut into the back of the bottom electrode surrounding the central contact. This groove extended to within 5 mm of the front surface. The guard metallization was continued to the groove which was then coated with a thin conductive silver paint. This groove will then intercept any field lines between the central wire

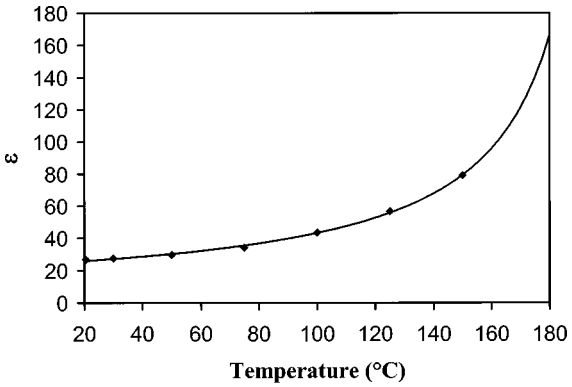

FIG. 2. Ferroelectric behavior of Zerodur. ϵ vs temperature for Zerodur measured at 1 kHz with the capacitance bridge used for the thickness measurements. Note that the solid line is a fit to the data with the Curie–Weiss law with a T_c of 206 °C. The error bars correspond to the best estimate of two standard deviations in the experimental uncertainty.

contact through the guard gap to the high electrode. It is probable that this modification would allow the use of a Zerodur electrode, but we stayed with fused quartz as a cautionary procedure.

B. Electrode holder

In order to realize the maximum accuracy with the electrode, a sample holder was designed to both eliminate any stray capacitative coupling in the bridge leads, when used as a three-terminal device and also to minimize any thermally induced strains on the electrodes. The potential for interference by thermal strain is shown by the observation that the weight of a small tissue wiper placed on top of the top electrode created a noticeable change in the measured capacitance.

The holder, shown in cross section in Fig. 3, had a land machined in it so that the bottom electrode could simply rest on it without any applied force. The circumference of the electrode had three small subdrills so that set screws in the holder could be inserted into them again without any applied force. These screws were provided as a safety when handling

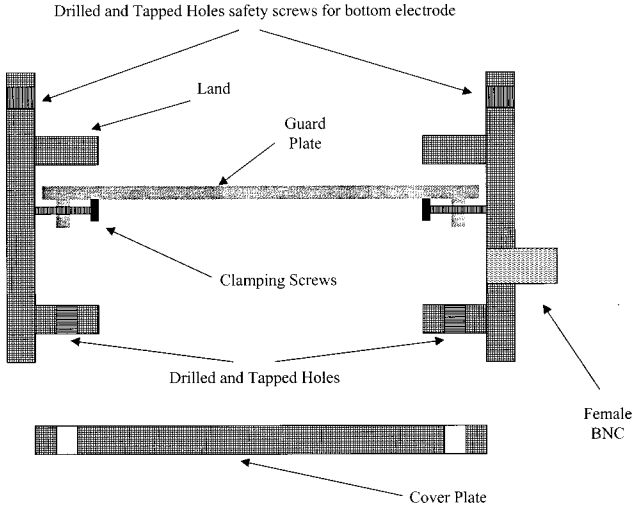

FIG. 3. Schematic of the capacitance cell holder.

the cell to prevent the electrode from falling out of the holder. The coaxial bridge low lead was made from Teflon insulated cable and attached at one end to a BNC receptacle in the holder using high temperature solder with a melting point above 250 °C. The other end was clamped to a shield plate placed between it and the bottom of the electrode was held in place by clamp screws against the wall of the holder. Fine 30 gauge wire coils were used to complete the contact to the electrode to eliminate any thermally induced strains from the Teflon insulation of the cable. Actual connection was made by a push-on connection using center female contacts from 50 Ω BNC connectors.

A miniature semirigid copper clad coaxial line clamped to the side of the holder was used to make contact with the top electrode. This lead overhung the electrode and also made contact through a fine copper coil. This coil did not need any shielding as the connection to the bottom electrode was completely shielded from it by the holder. In this way all thermally induced strains from the connections could be minimized without compromising the necessary shielding.

C. Sample preparation

The electrodes are designed to be separated by three pieces of sample placed between the bottom guard ring and the top electrode (see Fig. 1). Since a three-terminal measurement is made such that capacitances to guard and ground are eliminated, this removes the sample from the capacitance measuring path and, hence, one does not need to know the sample's dielectric constant.

However, since the electrodes are optically flat, care does have to be used when placing the sample between the electrodes. The sample must be carefully cleaned and the electrodes assembled in a dust-free environment. Also, any residual air layers must be removed.

Therefore, the following protocol was followed prior to each run. In a laminar flow hood equipped with a high efficiency particle arresting (HEPA) filter, the electrode surfaces were cleaned with ethanol and distilled water and dried with lens tissue. High pressure filtered air was used to remove any remaining particles from the surface. All samples were cleaned in the same way. As is shown in Fig. 1, the samples were placed in the outside guard ring spaced $2\pi/3$ rad apart. The entire cell apparatus was then placed in a vacuum oven at 25 °C under 4.0 kPa of vacuum for 1 h. (Evacuation of the cell was found necessary to simulate wringing, i.e., the removal of a trapped air layer caused by the contact of optically smooth surfaces. This phenomena has been noted previously.[7]) The cell was then transferred to a Tenney humidity/temperature chamber. The cell was equilibrated about 10 °C above the highest temperature of interest. It is important to note that the humidity/temperature chamber was equipped with a dry air purge with a manufacturer's quoted dew point of −90 °C (this corresponds to a vapor pressure of 9.3×10^{-3} Pa). Therefore, all thermal expansion measurements were performed effectively at a relative humidity of 0%.

D. Capacitance measurement

The capacitance between the plates was measured using a commercial automated three-terminal capacitance bridge which uses an oven-stabilized quartz capacitor and has a stated stability and relative standard uncertainty of better than $\pm 10^{-8}$ pF/pF for the range of capacitances used with this cell (Andeen–Hagerleen 2500A 1 kHz Ultra-Precision capacitance Bridge).[11] The major inaccuracy for length measurement purposes is the guard gap error, however, the best theoretical evaluation of this error using the estimated gap width and its variation with distance shows that this is not a factor for the measurement of thermal expansion.[8] This is because the variation in the gap correction varies quite slowly with distance and even samples with large values of thermal expansion do not change their length by more than several percent over the measured range of temperatures.

During the course of the experiment, random temperatures were sampled to eliminate any systematic errors induced by heating and cooling. The cell was allowed to equilibrate at any given temperature until the relative fluctuations in the vacuum corrected capacitance were no more than 10^{-6} pF/pF. The barometric pressure was monitored during the run. The temperature of the cell was calibrated in terms of the chamber temperature with a resistance temperature device (RTD) mounted to the cell with thermally conducting paste. The RTD was calibrated against a National Institute of Standards and Technology (NIST) certified ITS-90 standard reference thermometer.

E. Data reduction

Data reduction was performed in the following manner. In this article, all measurements were performed at approximately 0% relative humidity. (In the second article in this series, we will demonstrate the necessary corrections when operating under humid conditions.) The vacuum corrected capacitance C_{vac} is obtained from the measured capacitance C through the dielectric constant of the medium separating the plates. In the experiments performed in this article, the medium is dry air. To obtain C_{vac} from C we use the relationship:

$$C_{\mathrm{vac}}=\frac{C}{\epsilon}, \tag{3}$$

where ϵ is the static dielectric constant of the material between the two plates. The molar polarization (P) of air obtained from the literature is $P=4.31601\times10^{-3}$ L/mol.[12] To calculate ϵ, P must be divided by the molar volume v given by the ideal gas law to be

$$v=\frac{RT}{p}, \tag{4}$$

where T is the temperature, p is the pressure, and R is the gas constant ($R=8.314507$ L kPa mol^{-1} K^{-1}).[13] A comparison was made between the molar volume obtained with the ideal gas law and with that of equation of state data[14] and it was determined that the error in ϵ was far less than the experimental uncertainty. From the value of the polarization, the static dielectric constant is obtained with the following equation:

$$\epsilon=\frac{2(P/v)+1}{1-(P/v)}. \tag{5}$$

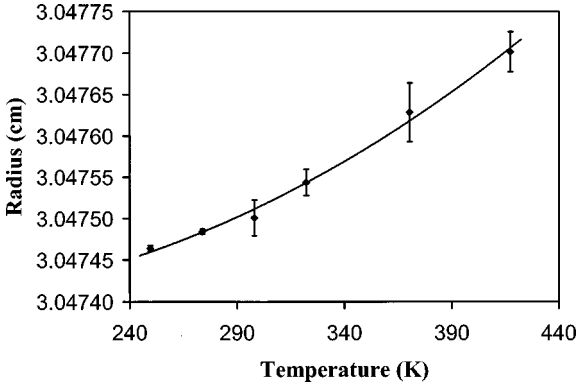

FIG. 4. Electrode radius as a function of temperature determined using 2.0 mm Zerodur spacers. Note that the diamonds correspond to averages over at least two different experiments at each temperature and that the error bars correspond to the best estimate of two standard deviations in the experimental uncertainty.

F. Electrode area calibration

From Eq. (2), it is apparent that the area of the electrode must be calibrated as a function of temperature. To achieve this goal, spacers were made from Zerodur[11] with a thickness of approximately 2.0 mm. The actual dimensions of the Zerodur spacers were measured in a ball to plane configuration with a specially designed caliper equipped with a linear voltage displacement transducer (LVDT) that had a resolution of $\pm 1\times10^{-4}$ mm. The spacers were treated in the same manner as is described in the sample preparation section. The Zerodur was then run at -25, 0, 25, 50, 100, and 150 °C with each temperature being sampled twice. From the average value of the spacer thickness and the vacuum corrected capacitance C_{vac} at room temperature, the electrode area (A) was determined. Subsequent measurements accounted for the slight expansion/contraction ($\alpha_{\mathrm{Zerodur}}=0.05\times10^{-6}$ K^{-1}) of the Zerodur. The results of the radius of the electrode (r_T) as a function of temperature (T) are shown in Fig. 4. It was determined that this data set was well described by a quadratic equation of the form

$$r_T=(3.3432\times10^{-9}\ \mathrm{cm/K^2})T^2 -(7.6071\times10^{-7}\ \mathrm{cm/K})T+3.047441\ \mathrm{cm}. \tag{6}$$

If Eq. (6) is converted to units of $\Delta r/r_{25}$, where r_{25} is the electrode radius at 25 °C and Δr is (r_T-r_{25}), and differentiated with respect to T, the coefficient of thermal expansion of the fused quartz electrode (α_{fq}) is obtained:

$$\alpha_{\mathrm{fq}}=(2.2\times10^{-9}\,\mathrm{K^{-2}})T-2.5\times10^{-7}\,\mathrm{K^{-1}}. \tag{7}$$

This value can be compared to the values obtained by Kikuchi and co-workers[15] on vitreous silica. However, it must be recalled that vitreous silica (or fused quartz) is produced by several different methods and the CTE depends upon which

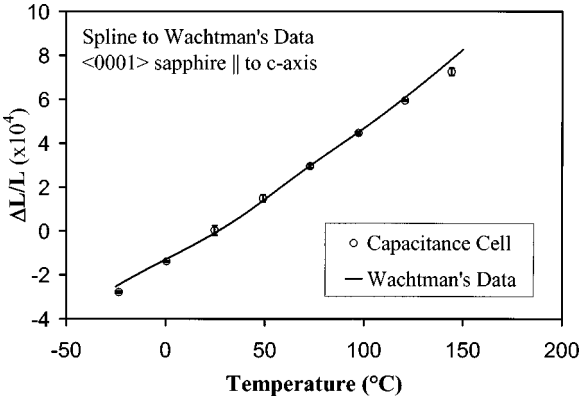

FIG. 5. Single crystal $\langle 0001 \rangle$ Al_2O_3 (sapphire) expansion as a function of temperature. The solid line is a spline to the data from Ref. 16. Note that the open circles correspond to averages over at least two different experiments at each temperature and that the error bars correspond to two standard deviations in the experimental uncertainty.

method was utilized. As we are uncertain as to how our fused quartz was produced, we will compare our results to the results of Kikuchi and co-workers at 400 K where all of the different types of vitreous silica have the same CTE of approximately $0.65\times10^{-6}\,\mathrm{K}^{-1}$. The solution of Eq. (7) with $T=400\,\mathrm{K}$ yields a value for α_{fq} of $0.63\times10^{-6}\,\mathrm{K}^{-1}$. Our value is within the experimental error of Kikuchi and co-workers, and therefore we feel confident that our calibration curve is valid.

G. Sample measurements

Two different samples were measured to demonstrate the capabilities of the capacitance cell. The first sample, 0.5 mm single crystal, $\langle 0001 \rangle$ oriented Al_2O_3, was measured to demonstrate the ability of the technique to produce the expansion curve of a known material. The second sample, 14 μm thick Cyclotene[11] (a bis-benzocyclobutene based material) film obtained from Dow Chemical Company, was chosen to demonstrate the ability of the cell to measure the expansion of thin polymeric films.

IV. RESULTS AND DISCUSSION

A. $\langle 0001 \rangle$ oriented aluminum oxide (alumina/sapphire)

In Fig. 5, we have plotted $\Delta d/d_{25}$ for our experimentally determined data on single crystal $\langle 0001 \rangle$ oriented aluminum oxide. To compare our values to those in the literature, we obtained the raw data of Wachtman and co-workers.[16] These data were then fit to a 10 knot cubic spline.[17] Wachtman and co-workers obtained their data at 10° and 90° to the *c* crystallographic axis (principal axis). Therefore since our data were obtained parallel to the *c* axis the following relationship given by Wachtman and co-workers[18] was utilized:

$$\alpha_{\parallel}=\frac{\alpha_{\psi}-\alpha_{\perp}\sin^2\psi}{\cos^2\psi}, \tag{8}$$

where a_{ψ} is the expansion coefficient at an angle ψ, $\alpha_{\parallel}$ is the expansion coefficient parallel to the principal axis, and $\alpha_{\perp}$ is the expansion coefficient perpendicular to the principal axis. Since these are isothermal measurements, the αs in Eq. (8) can be replaced by the appropriate $\Delta d/d$. Following Wachtman and co-workers,[18] 1.34×10^{-4} was subtracted from the values for the parallel value of $\Delta d/d$ to convert the data to a reference temperature of 25 °C. These data are the curve shown in Fig. 5.

Our data agree rather well with the previous data set, with the exception of the deviations at −25 and 150 °C. However, the deviation at −25 °C should be considered in light of the fact that Wachtman and co-workers used two different experimental setups and their data were then matched at 25 °C. Examination of the spline to Wachtman and co-worker's data shows that the curvature in our data is much smoother than that of Wachtman and co-workers indicating that our data are more self-consistent. One other fact which makes our data set superior to that of Wachtman and co-workers is the temperature expanded uncertainty of ±1.4 K associated with their data, compared to our temperature expanded uncertainty of ±0.2 K. (Throughout this article, quoted uncertainties represent the best estimate of two standard deviations in the experimental uncertainty.)[19] We have been unable to determine the cause for the deviation at 150 °C, although it is possible that there was a small amount of moisture in the chamber. Calculations indicate that a relative humidity of approximately 0.3% is sufficient to cause the deviation at 150 °C. Since calibration of the humidity sensor was performed only to 100 °C, this remains a possibility. This issue will be examined further in a forthcoming article. However, this deviation is small enough that it would not affect the measurement of polymer films.

It should be recalled that excluding problems associated with asperities in the films, our technique gives the same relative resolution in thickness regardless of the absolute thickness. It is important to realize that we have resolved the expansion of single crystal alumina which has an expansion coefficient on the order of $3\ \mu\mathrm{m\,m^{-1}\,K^{-1}}$. If this is compared to polymer films which have expansion coefficients at least an order of magnitude larger, it is apparent that polymer films will be far easier to resolve.

B. Cyclotene film

Due to the extreme sensitivity of our technique, we were able to resolve creep of the sample at levels that ordinarily would not be observable. Figure 6 shows the thickness versus time plot at 60 °C. There are several different ''regimes'' in the plot. The rapid rise (or fall if the temperature jump was performed in the opposite direction) at short times is due to thermal equilibration, the duration of which agrees well with the equilibration time followed by thermometry. This equilibration time is followed by a steady decrease in film thickness (l) until a plateau is reached in which the film thickness is not changing with time (t). The plateau extends further beyond what is shown in Fig. 6. (It should be noted that we use l and d interchangeably since l refers to sample thickness and d refers to capacitor plate separation.)

To remove the effects of creep, the following protocol was followed. A derivative plot was made (Fig. 7) to find the inflection point where thermal conductivity equilibration

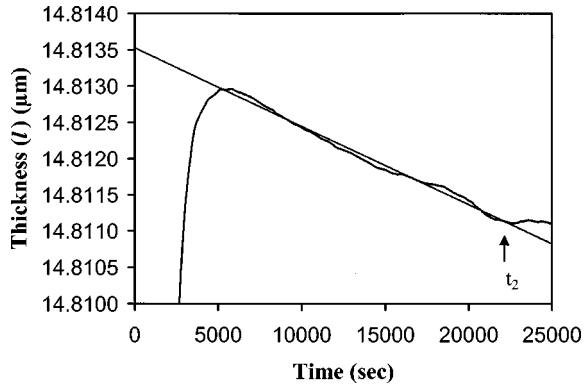

FIG. 6. Thickness (l) vs time for Cyclotene at 60 °C after equilibration at 25 °C. (The best estimate of two standard deviations in the experimental uncertainty is ±0.02 nm.)

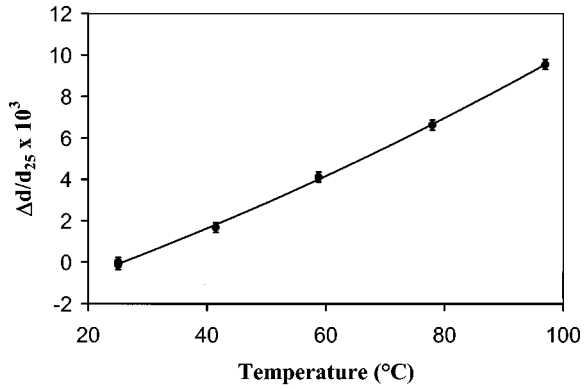

FIG. 8. Expansion curve ($\Delta d/d_{25}$ vs T) for Cyclotene. Note that the error bars correspond to two standard deviations in the experimental uncertainty as were estimated from the two experiments performed at 25 °C.

stops and creep begins (i.e., a plot of $\Delta l/\Delta t$ vs t, where the Δt corresponded to the 10 s spacing between measurements). The point at which this curve crosses the t axis is taken as the beginning of the creep t_1. Because the thickness changes by small amounts over large periods of time, the creep is indistinguishable from noise in the derivative plot. The point at which the plateau is reached is taken as the end of the creep t_2. This is then extrapolated to $t=0$ with a linear fit to the entire data set from t_1 to t_2 (Fig. 6).

To verify the consistency of the sample measurement, the following temperature profile was utilized. Initially, the sample was equilibrated at 150 °C for 20 h. After the relative vacuum corrected capacitance varied less that 1 μF/F, the cell was again equilibrated with the same tolerance condition at the following temperatures (in the following order): 100, 25, 60, 40, 80, and 25 °C. The data at each temperature were corrected for creep and the curve in Fig. 8 was obtained. The error bars in Fig. 8 are estimates of the uncertainty in the experimental data obtained from the two runs at 25 °C. It is apparent from Fig. 8 that the data are self-consistent as they fall on the same line, within the experimental uncertainty. Furthermore, it is apparent the data at 25 °C agree well in light of the fact that the material's dimensions changed throughout the entire experiment. The difference in thickness between the two measurements at 25 °C is 0.2±0.02 nm. This difference could be reduced by performing the measurements in a series of equally spaced temperature steps with the same measurement and creep ''removal'' procedure as described above. Our random temperature sampling, although demonstrating the self-consistency of the measurements, introduces uncertainties due to a varying thermal lag time which results in a cumulative error problem. It should be noted however, that the results obtained for the expansion coefficient by our capacitance cell agree reasonably well with those obtained at Dow Chemical Company by a combination of TMA and volumetric dilatometry measurements.

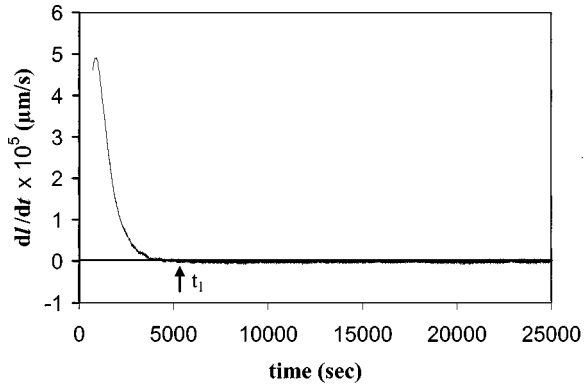

FIG. 7. Derivative plot (dl/dt vs t) for Cyclotene at 60 °C after equilibration at 25 °C. The time at which the curve has reached a value of zero is the value for t_1, the starting point for the linear extrapolation to zero. Recall that the change in time (dt) corresponds to a 10 s period so that changes over long periods of time are not observed. (Note that the best estimate of the combined standard uncertainty with a coverage factor of 2 is ±0.04 nm/s.)

C. Silicon

We feel it germane to mention one inherent problem in the current design of the capacitance cell. Measurements cannot be made on silicon or on materials on a silicon substrate. The reason is that silicon and nichrome form a Schottky barrier and act as a voltage rectifier. Because of the nature of the interface, this takes the measuring frequency of 1 kHz and increases it to the ultrasonic level which in turn causes the epoxy contacts to be shaken loose. The solution, if needed, is quite simple. The top electrode can have a guard ring added such that the inner electrode area is larger than that of the lower electrode. If the samples are kept on the guard rings of both electrodes, the silicon is held at zero potential and no voltage rectifier will be formed. As the upper electrode area is larger, the bottom electrode will still be the defining area for Eq. (2).

D. Discussion of errors

1. Electrode tilt

An advantage of this cell is that the design is such that any uncertainties due to the small amount of tilt caused by sample variations will not significantly affect the results. By simple symmetry arguments, it can be shown that any deviations due to a lack of parallelism enter as the square of the tilt angle. For thin films placed between 5 cm diam plates,

the maximum possible angle is so small ($\sim 1\ \mu$m/5 cm) that any variation in this angle is well beyond any possible experimental resolution.

2. Thickness reproducibility

One source of error that is introduced from three pieces that are not of identical height arises if the sample pieces move during the course of the measurement. If the samples are not in the exact same location and orientation, the mean distance between the electrodes will change simply due to the geometry. This source of error is minimized by eliminating all sample motion relative to the electrodes. Furthermore, excess vibration should be eliminated as this can introduce a time dependent thickness variation.

We have previously mentioned that the sample is wrung prior to measurement by applying a vacuum. This source of uncertainty was shown by preliminary work with an older electrode design to be gradually reduced by repeated temperature cycling. Our best estimate for the total magnitude of the wrung layer is derived from the measurements on $\langle 0001 \rangle$ single crystal Al_2O_3. This sample was optically flat and sufficiently rigid that any additional sources of error are eliminated. Data taken upon first insertion of the samples to the final thickness give an estimate of greater than 40 nm for the combined top and bottom interfaces. However, proper sample handling and conditioning have been shown to eliminate this source of error.

Another source of error is that due to creep. For samples approximately 1 cm^2 in total area, the applied stress with our current top electrode is 0.02 MPa. For many materials, such as filled epoxy resins and polyimides, there is no observable creep near 25 °C and low humidities. However, especially at high temperatures and humidities, the sample can creep, as shown by a downward drift in the total distance after thermal equilibration is achieved. In addition, there can be dimensional relaxation as well as diffusion controlled moisture absorption, all on longer time scales than that due to thermal equilibration. Ultimately, these-dimensional changes will set the limit as to how well thermal expansion can be defined. For slow variations, such as those observed in the Cyclotene sample, back extrapolation to the beginning of the temperature jump and taking the difference from readings just prior to the jump will minimize this source of uncertainty. Since this is a material based limit, this uncertainty must be estimated for each sample individually and is not due to the measurement cell.

Similarly, any warpage can interfere with the actual measurement. For composite samples with layers of different CTEs in the plane of the sample, warpage can become a problem. This is one case where increased load could help. However, we have seen a highly stressed sample that formed visible wrinkles over a narrow temperature range. This was manifested as a sudden jump in sample thickness.

Finally, sample flatness becomes an increasing problem with the anisotropic materials. For some liquid crystal polyimides, the thermal expansion can be close to zero in the xy plane while near $100\times10^{-6}\,K^{-1}$ in the thickness direction. For these materials, sample flatness will become the limit to the estimation of the CTE perpendicular to the xy plane. For materials that are not highly anisotropic, this source of uncertainty becomes less important and in the limit of an isotropic material, the orientation and shape of the sample do not matter.

ACKNOWLEDGMENTS

The authors wish to thank Dr. E.O. Shaffer II of Dow Chemical Company for providing them with the Cyclotene material and D. Wilmering for production of the capacitance cell and technical support. One of the authors, C.R.S., would like to acknowledge the support of the NIST-NRC Postdoctoral Research Associate Program.

[1] W. Wu, J. H. Van Zanten, and W. J. Orts, Macromolecules **28**, 771 (1995).
[2] J. L. Keddie, R. A. L. Jones, and R. A. Cory, Europhys. Lett. **27**, 59 (1994).
[3] P. S. Ho, T. W. Poon, and J. Leu, J. Phys. Chem. Solids **55**, 1115 (1994).
[4] *Annual Book of ASTM Standards*, edited by R. A. Storer (American Society for Testing of Materials, West Conshohocken, PA, 1997), Vol. 14.02, p. 548.H.M.
[5] G. D. Sao and H. V. Tiwary, J. Appl. Phys. **53**, 3040 (1982).
[6] H. N. Subrahmanyam and S. V. Subramanyam, J. Mater. Sci. **22**, 2079 (1987).
[7] H. M. Tong, H. K. D. Hsuen, K. L. Saenger, and G. W. Su, Rev. Sci. Instrum. **62**, 422 (1991).
[8] J. I. Lauritzen, Jr., 1963 Annual Report Conference on Electrical Insulation, NAS-NRC Publ. 1141.
[9] M. Schen, F. I. Mopsik, W. Wu, W. E. Wallace, N. C. Beck Tan, G. T. Davis, and W. Guthrie, Polym. Prepr. (Am. Chem. Soc. Div. Polym. Chem.) **37**, 180 (1996).
[10] Schott material having a coefficient of thermal expansion of less than $0.05\times10^{-6}\,K^{-1}$.
[11] Certain commercial materials and equipment are identified in this article in order to specify adequately the experimental procedure. In no case does such identification imply recommendation or endorsement by the National Institute of Standards and Technology, nor does it imply that the items identified are necessarily the best available for the purpose.
[12] A. A. Maryott and F. Buckley, Table of Dielectric Constants and Electric Dipole Moments of Substances in the Gaseous State, NBS Circular 537, 1953.
[13] E. R. Cohen and B. N. Taylor, Phys. Today **50**, BG7 (1997).
[14] V. V. Sychev, A. A. Vasserman, A. D. Kozlov, G. A. Spiridonov, and V. A. Tsymarny, *Thermodynamic Properties of Air* (Hemisphere, New York, 1987).
[15] Y. Kikuchi, H. Sudo, and N. Kuzuu, J. Appl. Phys. **82**, 4121 (1997).
[16] J. B. Wachtman Jr., T. G. Scuderi, and G. W. Cleek, ADI Auxilliary Publications Project, Photoduplication Service, Document No. 7146, Washington, D.C.: Library of Congress, 1962.
[17] J. H. Ahlberg, E. N. Nilson, and J. L. Walsh, *The Theory of Splines and Their Applications* (Academic, New York, 1967).
[18] J. B. Wachtman, Jr., T. G. Scuderi, and G. W. Cleek, J. Am. Ceram. Soc. **45**, 319 (1962).
[19] B. N. Taylor and C. E. Kuyatt, Guidelines for Evaluating and Expressing the Uncertainty of NIST Measurement Results, Natl. Inst. Stand. Technol. Note 1297, US Govt. Printing Office, Washington, D.C. (1995).